J. Phys. Chem. A **2000,** *104,* 1915−1919

An AM1 Study of the Reaction of Ozone with C_{60}

Zhenfeng Shang,[†] Yinming Pan,[†] Zunsheng Cai,[†] Xuezhuang Zhao,*,[†] and Auchin Tang[†,‡]

Department of Chemistry, Nankai University, Tianjin, 300071, People's Republic of China, and
Institute of Theoretical Chemistry, Jilin University, Changchun, 130023, People's Republic of China

Received: September 29, 1999; In Final Form: December 3, 1999

Semiempirical molecular orbital calculations have been carried out on the ozonization of C_{60} in order to obtain information on possible reaction paths and products. Stationary points involved in the proposed mechanism and their harmonic vibrational frequencies have been calculated at the AM1 level of theory. The computational results shown that not only from a thermodynamic point of view but also from a kinetic point of view the O_3 was most likely added on the 6/6 bond of C_{60}. In the ozonization mechanism of C_{60}, the 1,3-dipole addition of O_3 to C_{60} is the rate-determining step and the major product is $C_{60}O$ with epoxide functionality.

1. Introduction

The fullerene oxides are interesting materials for the formation of other fullerene-based entities. Many methods have been used to produce fullerene oxides, including photooxygenation,[1,2] electrochemical oxidation,[3] and ozonization.[4−7] Ozonization of C_{60} is a facile way to produce fullerene oxides. The experimental results[5−7] show that the reaction of C_{60} with ozone results in the formation of $C_{60}O$ which reacts further to produce $C_{60}O_2$ and so on because C_{60} contains 30 formal double bonds, and hence facile ozonization of C_{60} is expected.

A lot of work has been done to elucidate the mechanism of ozonization of olefins; however, it has not been all clarified yet. Criegee[8,9] provides the generally accepted mechanism, which involves three distinct steps. In the first, ozone adds directly to the olefin to form a cyclic adduct(I). This then dissociates to a mixture of a carbonyl compound and a carbonyl oxide (III) which then recombine to form the ozonide(IV). In recent years, a number of theoretical studies on the mechanism of the ozonolysis have been appearing.[10−21] They calculated the heats of formation of the various stable intermediate and transition states involved. The inclusion of electron correlation is absolutely required to make ab initio calculation reliable. However, the larger members of the series prevents the use of ab initio methods completely; therefore, ab initio calculations either dealt only with some individual steps and not with the whole reaction sequence[15−17] or accomplished partial rather complete geometry optimization.[12,13,15,19] The comprehensive quantum chemistry study of the Criegee mechanism to date appears to have employed exclusively semiempirical methods.[14,21] (See Figure 1.) Recently, J. M. Anglada et al.[22] reported a systematic theoretical study of ozonolysis of ethylene by high-level ab initio method. The energy barrier they obtained is comparable with the reported experimental value.

Unlike olefins, the spherical nature of C_{60} places stringent steric constraints on the conversion of the molozonide intermediate to the ozonide, and raises questions about the fate of the initial adduct. In this study we discuss the application of AM1 method to the elucidation of this aspect. A modified Criegee mechanism, i.e., the mechanism of ozonization of C_{60}, has been suggested and various transition states and intermediates involved in the process have been studied.

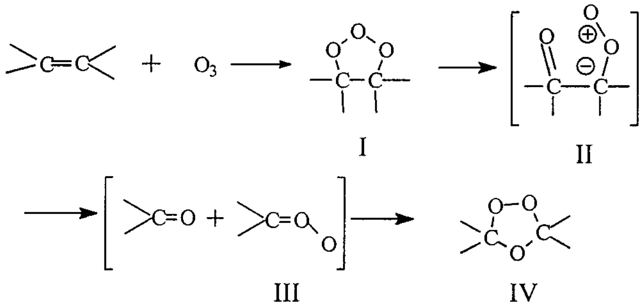

Figure 1. The Criegee's mechanism of ozone with olefins.

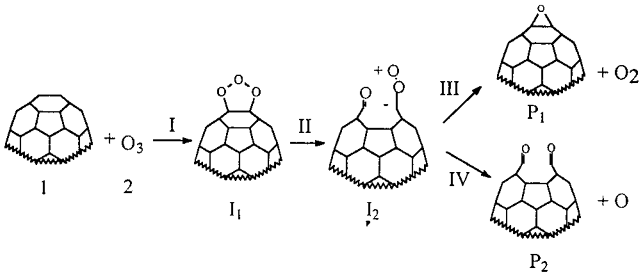

Figure 2. The proposed mechanism of ozonization of C_{60}.

2. Computational Methods

The size of the system studied prevents the use of ab initio molecular quantum mechanical methods. Therefore, all calculations presented here were performed with the AM1 semiempirical method[23] as implemented in the MOPAC7.0 program package.[24] The AM1 method has been preferred over other semiempirical methods due to three main reasons: first, it yields reliable results for the geometries of C_{60}[25] and C_{70}; second, for the ozonolysis of olefins, it reproduces high-level ab initio calculations and experimental results;[21,22] and third, Dewar's group encourages the use of the AM1 method among other semiempirical methods for the study of pericyclic reactions.[26]

---

* Corresponding author. E-mail: Zhaoxuezhuang@263.net.

[†] Department of Chemistry.

[‡] Institute of Theoretical Chemistry.

10.1021/jp9934937 CCC: $19.00

TABLE 1: Major Calculated Bond Length (B.L., unit: nm) and Bond Order (B.O.) of Transition State and Primary Ozonide in the Addition of O_3 to C_{60}

	C1−C2		C1−O1′		C2−O3′		O1′−O2′		O2′−O3′	
	B.L.	B.O.	B.L.	B.O.	B.L.	B.O.	B.L.	B.O.	B.L.	B.O.
6/6TS$_1$	0.1431	1.28	0.2018	0.31	0.2018	0.31	0.1197	1.30	0.1197	1.30
6/6PO	0.1588	0.90	0.1456	0.95	0.1456	0.95	0.1307	0.99	0.1307	0.99
6/5TS$_1$	0.1507	1.04	0.1673	0.52	0.2271	0.19	0.1233	1.17	0.1177	1.34
6/5PO	0.1637	0.87	0.1452	0.95	0.1452	0.95	0.1306	0.99	0.1306	0.99

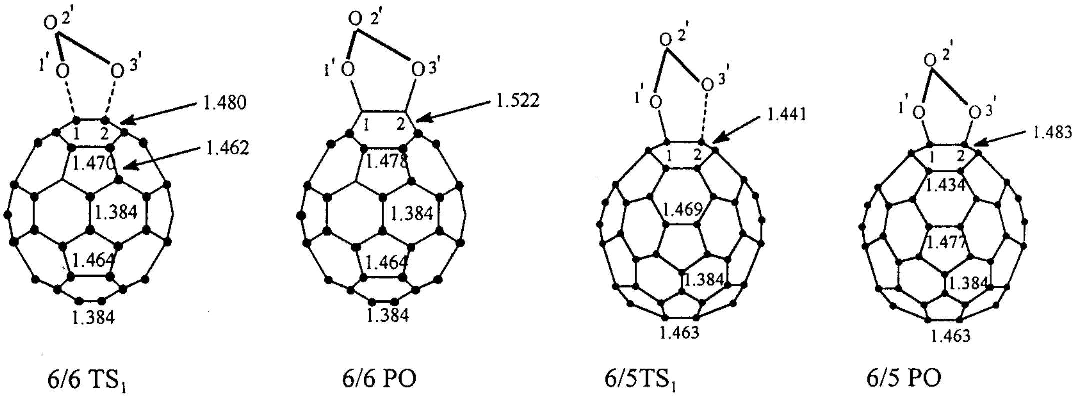

6/6 TS$_1$ 6/6 PO 6/5TS$_1$ 6/5 PO

Figure 3. AM1 optimized geometries of primary ozonide and transition states in the reaction of O_3 with C_{60}.

Harmonic frequency analysis verified the nature of the stationary points as minima (all real frequencies) or as transition structures (with one imaginary frequency).

3. Results and Discussion

According to part of the Criegee mechanism and the experimental results, we suggested the mechanism of ozonization of C_{60} as shown in Figure 2.

In Figure 2, 1 and 2 refer to the reactant C_{60} and O_3, I_1 and I_2 are two intermediates, and P_1 and P_2 are two kinds of possible products. Roman numerals I, II, III, and IV indicate reaction steps. Four steps are involved in this mechanism: (1) the formation of intermediate 1 (I_1), also known as the primary ozonide (PO), by a 1,3-cycloaddition process. (2) Intermediate 1 dissociates to intermediate 2 through the breaking down of C−C bond in C_{60}. (3) The intermediate 2 converted to $C_{60}O$ (P_1) with epoxide functionality or $C_{60}O_2$ (P_2) with ketone functionality.

3.1. Structures of Transition States and Products of 1,3-Dipole Adduct. Similar to the ozonization of olefins, the first step of the reaction between ozone and C_{60} involves the formation of 1,2,3-trioxolane, also known as the primary ozonide (PO), by a 1,3-dipole addition process. As we have known that C_{60} has two kinds of bonds, i.e., 6/6 and 6/5 bonds, and hence there will have been two kinds of POs that we called 6/6 PO and 6/5 PO, respectively.

The AM1 optimized geometries, which are depicted in Figure 3, can be labeled as transition state of 6/6 PO (6/6 TS$_1$) and 6/5 PO (6/5 TS$_1$). The structure parameters of transition states and POs are given in Table 1. No symmetry constraint has been imposed on the C_{60}−O_3 system, however, the resulted transition state in the 6/6 addition (6/6 TS$_1$) has a C_s symmetry structure. The bond lengths of the two forming C−O bonds in 6/6 TS$_1$ are 0.2018 nm and their bond order are 0.31. With regard to compare, we also studied the transition states and products of O_3 reaction with ethylene and benzene. Similar results have been found in the reaction of O_3 with ethylene and benzene. Their transition states also have C_s symmetry, and the two forming C−O bonds are 0.206 and 0.196 nm, respectively.

TABLE 2: Bond Angles and Dihedral Angles of Transition States and Primary Ozonides

	D_{OOCC}	D_{OCCO}	∠OOO	∠$O_{1'}C_1C_2$
6/6 TS1	27.40	0.24	114.81	98.33
6/5 TS1	26.94	0.38	114.58	105.40
6/6 PO	22.16	0.31	107.96	100.37
6/5 PO	22.45	0.83	108.26	99.75

The bond length of C1−C2 in the 6/6 TS$_1$ is 0.1431 nm, which is closer to the corresponding bond in the addition of O_3 to benzene (0.1435 nm) and longer than that of O_3 to ethylene (0.1375 nm). The longer bond distance in the 6/6 TS$_1$ may be ascribed to the longer C1−C2 bond of the C_{60} molecular than the C═C bond of an ethylene molecular in an isolated state.

The C1−C2 bond of the reaction sites in the 6/6 PO has been pulled away from the remaining part of the C_{60} sphere, having a very long bond distance, 0.1588 nm. Its bond order is reduced from 1.49 (in original C_{60}) to 0.9. These results indicate that the C1−C2 bond in the 6/6 PO has completely been converted to single bond. The corresponding bonds in the products of ethylene and benzene follow a similar trend, i.e., they also have been converted to single bonds.

Unlike 6/6 addition there is an unsymmetrical transition state in the 6/5 addition. The bond lengths of the newly formed C1−O1′ and C2−O3′ bonds are 0.1673 and 0.2271 nm, and their bond orders are 0.52 and 0.19, respectively. This indicate that the bond between C1−O1′ is stronger; however, the bond between C2−O3′ is weaker. The reason of forming unsymmetrical transition state may be due to the longer bond length of 6/5 bond than that of 6/6 bond in C_{60}. If a symmetry one was formed then both of the C1−O1′ and C2−O3′ bonds would be very weak because of the little overlap between these atoms. It must be noted that the AM1 calculations predict the concerted and synchronous transition state for 6/6 addition and the concerted and unsynchronous transition state for 6/5 addition.

It can be seen from bond lengths labeled in Figure 3 that the influence of interactions upon the geometry is limited to the local area in the addition of O_3. The single bonds and double bonds in the C_{60} sphere away from the reaction sites are not much distorted from their original bonds of C_{60}, 0.1384 and 0.1464 nm, respectively. The bond angles (∠) and dihedral

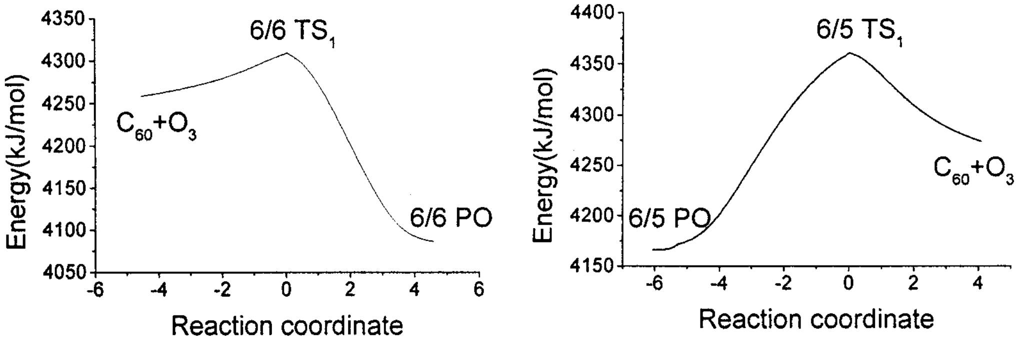

Figure 4. Figure 4. The intrinsic reaction coordinate of O_3 added to 6/6 and 6/5 bonds.

TABLE 3: Calculated Heats of Formation($\Delta H_f°$) of Reactants, Transition States, and Products at 25 °C for the Ozonization of C_{60}, together with Heats of Reaction (ΔH_r), Activation Energy($\Delta H^‡$), Activation Energy of Retroaddition ($\Delta H^‡_r$), Deformation Energy Needed to Distort Reactant C_{60}(ΔH_{def}^{C60}) and O_3(ΔH_{def}^{O3}) at Their Geometry in the Transition State and Interaction Energy (ΔH_{int}) (unit: kJ mol^{-1})

	reactants		TS_1		adducts	
	C_{60}	O_3	6/6	6/5	6/6	6/5
$\Delta H_f°$	4072.3	158.2	4314.1	4365.6	4089.4	4170.2
ΔHr					−141.0	−60.2
$\Delta H^‡$			84.1	135.1		
$\Delta H^‡_r$			225.1	195.0		
ΔH_{def}^{C60}			15.1	35.1		
ΔH_{def}^{O3}			15.9	25.9		
ΔH_{int}			53.1	74.1		

TABLE 4: Calculated Heats of Formation ($\Delta H_f°$) of Reactants, Transition States, and Products at 25 °C for the Ozonization of Ethylene and Benzene, together with Heats of Reaction (ΔH_r), Activation Energy ($\Delta H^‡$), Activation Energy of Retroaddition ($\Delta H^‡_r$), Deformation Energy Needed to Distort Reactant (ΔH_{def}^r) and O_3 (ΔH_{def}^{O3}) at Their Geometry in the Transition State and Interaction Energy (ΔH_{int}) (unit: kJ mol^{-1})[a]

	$\Delta H_f°$	ΔH_r	$\Delta H^‡$	$\Delta H^‡_r$	ΔH_{def}^r	ΔH_{def}^{O3}	ΔH_{int}
reactants							
O_3	158.2						
ethylene	69.0						
1,3-butadiene	125.1						
benzene	92.0						
TS							
ethylene	274.9		47.7	251.5	14.6	15.9	17.2
1,3-butadiene	342.3		59.4	233.5	19.2	17.2	23.0
benzene	368.2		118.0	171.5	39.3	28.9	49.8
adducts							
ethylene	23.4	−203.8					
1,3-butadiene	108.8	−174.5					
benzene	196.6	−53.6.					

[a] The activation energy (47.7 kJ mol^{-1}, also in ref 21) of ethylene calculated by AM1 methods are larger than those of values yield by ab initio[22] (24.3 kJ mol^{-1}) and experiment[32] (17.4−25 kJ mol^{-1}). However, the heat of reaction of ethylene (−203.8 kJ mol^{-1}) is comparable with the ab initio[22] (−205.9 kJ mol^{-1}) and experimental value[34] (−163.2 kJ mol^{-1} to −213.4 kJ mol^{-1}). Therefore, AM1 methods overrate the activation energy and give much better value of heat of reaction for studying ozonolysis of olefins.

angles (*D*) are given in Table 2. Inspection of Table 2 reveals that both transition states and primary ozonides have oxygen envelope structures, which are in agreement with experimental[27−29] and theoretical[14,19,21,22] studies of ozone addition to ethylene.

Calculations following the intrinsic reaction coordinate (IRC)[30] for 6/5 TS_1 and 6/6 TS_1 have shown a monotonic decrease in energy and resulted in the formation of the suggested products and reactants (in reverse following). No distinct intermediates or second transition structures were found. This result confirmed our calculation is correct. (See Figure 4.)

The heats of formation of reactants, transition states, and products are collected in Table 3. Firstly, the heats of formation of adducts in this table show that from a thermodynamic point of view the 6/6 adduct is clearly preferred over the 6/5 adduct. In fact, as one can see from the activation energies, the 6/6 adduct is favored not only thermodynamically but also kinetically. The difference in the activation energy seems to be sufficiently large at present level of calculation to conclude that addition of ozone is most likely to occur on a 6/6 bond of C_{60}.

Secondly, to understand the origin of the differences between 6/6 and 6/5 ring junction attacks, the activation energy of each addition has been divided into deformation energy and interaction energy[25,31] ($\Delta H^‡ = \Delta H_{def} + \Delta H_{int}$). The deformation energy is taken as the energy needed to modify the geometries of the reactants to that they have in the TS, and is split into the deformation energy of reactants C_{60} (ΔH_{def}^{C60}) and O_3 (ΔH_{def}^{O3}). The interaction energy has three basic components, namely, the Pauli repulsion, the electrostatic interaction, and the orbital relaxation (polarization + charge-transfer effects). The deformation energy and interaction energy of reactants C_{60} and O_3 are also collected in Table 3.

It can be found from Table 3 that in 6/6 and 6/5 addition the deformation energy is smaller than interaction energy. The deformation energy and interaction energy in 6/6 addition are 31.0 and 53.1 kJ mol^{-1}, whereas in 6/5 addition they are 61.0 and 74.1 kJ mol^{-1}, respectively. From this fact we concluded that besides providing the energy needed to modify the geometries of the reactants that they have in the TS when forming the structure of the transition state, the activation energy mostly has been used to overcome the repulsion energy between the reactants. The deformation energy of C_{60} in 6/6 addition is smaller than that of 6/5 addition (they are 15.1 and 35.1 kJ mol^{-1}, respectively) indicated that the original geometry of C_{60} is changed slightly in the 6/6 addition. This may be accounted for the higher reactivity of 6/6 bond than that of 6/5 bond in C_{60}.

The transition states of O_3 reaction with ethylene, 1,3-butadiene, and benzene have also been studied to understand the reactivity characteristics of C_{60} with respect to those of other common aliphatic and aromatic hydrocarbons. The results are given in Table 4. The activation energy of ethylene and 1,3-butadiene are 47.7 and 59.4 kJ mol^{-1}, which is smaller than that of O_3 addition to 6/6 bond in C_{60} (84.1 kJ mol^{-1}). However, the activation energy of 6/5 addition is closer to that of benzene (118.0 versus 135.1 kJ mol^{-1}, respectively). These results indicate that the reactivity of 6/6 bond is lower than that of olefin but higher than that of benzene. The reactivity of 6/5 bond is closer to that of benzene.

TABLE 5: Bond Lengths (B.L., unit: nm) and Bond Order (B.O.) of TS$_2$ and I$_2$ Product in Reaction II

	C1−C2		C1−O1′		C2−O3′		O1′−O2′		O2′−O3′	
	B.L.	B.O.	B.L.	B.O.	B.L.	B.O.	B.L.	B.O.	B.L.	B.O.
TS$_2$	0.1628	0.82	0.1374	1.13	0.1476	0.91	0.1732	0.68	0.1197	1.26
I$_2$	0.2587	0.01	0.1221	1.97	0.1329	1.41	0.2579	0.01	0.1163	1.33

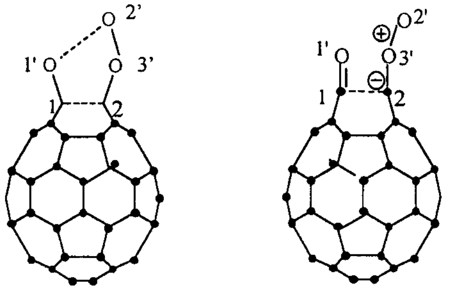

TS$_2$ I$_2$

Figure 5. The transition state and product of dissociation of molonozide.

TABLE 6: The Net Charge of C, O Atom in I$_2$

C$_1$	C$_2$	O$_{1'}$	O$_{2'}$	O$_{3'}$
0.304	−0.121	−0.193	−0.301	0.377

TABLE 7: Activation Energy, Heats of Reaction for Reaction II Calculated by AM1 Methods (Unit: kJ mol^{-1})

	$\Delta H_f°$	ΔH_r	$\Delta H^{\ddagger}$	$\Delta H^{\ddagger}_r$
I$_1$	4089.4			
TS$_2$	4147.6		58.2	95.4
I$_2$	4052.2	−37.2		

TABLE 8: Minimum-Energy Reaction Pathways Calculated Using AM1 for the Opening of the C2−O3′ bond

distance of C2−O3′ (nm)	AM1 energy (kJ mol^{-1})
0.145	0.0
0.16	23.76
0.17	54.43
0.18	87.61
0.19	119.62
0.20	148.70
0.21	174.14
0.22	194.72
0.23	212.13

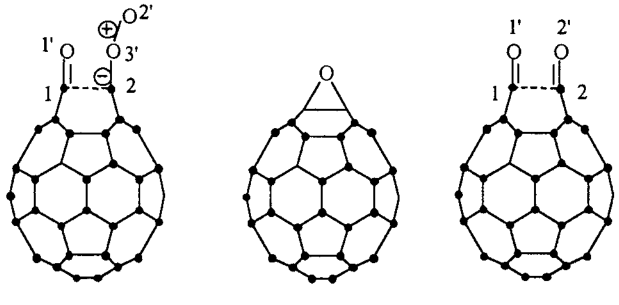

TS$_3$ P$_1$ P$_2$

Figure 6. The products and transition state in reactions III and IV.

The ozonization of C$_{60}$, olefin and benzene are exothermal reaction. The heats of reaction of O$_3$ added to 6/6 bond of C$_{60}$, ethylene, and 1,3-butadiene are larger than those of 6/5 bond and benzene. Therefore the 6/6 adduct, O$_3$−ethylene, and O$_3$−1,3-butadiene adduct are much more stable than those of 6/5 adduct and O$_3$−benzene adduct.

In the ozonization of olefin and benzene, the deformation energy of reactant is larger than the interaction energy. This fact indicates that in the formation of transition states of O$_3$ reaction with olefin and benzene the deformation of reactants is important and the activation energies are mainly used to modify the geometries of reactants. However in the reaction of O$_3$ with C$_{60}$, because there are more atoms in the C$_{60}$−O$_3$ system so that the repulsion energy between them is very large and the activation energy is mainly used to overcome it.

3.2. Dissociation of Molozonide. In the second step of ozonization of olefin, the C−C bond had been broken down and formed the zwitterionic intermediate II (Figure 1). This then dissociates to a mixture of a carbonyl compound and a carbonyl oxide III (Figure 1). Similar to olefin, the second step of ozonization of C$_{60}$ is also the bond rupture of C−C bond in primary ozonide and result in the formation of the zwitterionic intermediate 2 (I$_2$, Figure 2). However, C$_{60}$ has a stable spherical structure, and this prevents the molozonide intermediate from converting to the carbonyl compound and a carbonyl oxide.

The foregoing discussion suggests that not only from a thermodynamic point of view but also from a kinetic point of view, the O$_3$ was most possible added on the 6/6 bond of C$_{60}$. Therefore we only studied the formation of zwitterionic intermediate I$_2$ through the break down of C−C bond and the formation of final production of 6/6 isomer of molozonide.

Figure 5 shows the geometries of the transition state 2 (TS$_2$) and the I$_2$. Table 5 listed their bond lengths and bond order. Compared with its initial geometry, i.e., primary ozonide (I$_1$), the bond lengths of C1−C2 and O1′−O2′ in TS$_2$ increased 0.004 nm (0.1588 versus 0.1628 nm) and 0.0425 nm (0.1197 versus 0.1732 nm), their bond order decreased 0.08 (0.9 versus 0.82) and 0.31 (0.99 versus 0.68), respectively. These results indicated that these bonds have been breaking. Meanwhile, that the bond lengths of C1−O1′ and O2′−O3′ decreased and their bond order increased, indicated these bonds becoming stronger. In the I$_2$, the bond O1′−O2′ (bond length 0.2579 nm, bond order 0.01) and C1−C2 (bond length 0.2587, bond order 0.01) were broken completely and the C−O double bond between C1−O1′ were newly formed (bond length 0.1221 nm, bond order 1.966). The net charges of C, O atoms in I$_2$ (see Table 6) show that the product of molozonide dissociation is indeed zwitterionic intermediate. Reaction II is an inner molecular reaction, so it has lower activation energy, only 58.2 kJ mol^{-1}. This reaction is an exothermal reaction and its heats of reaction is 37.2 kJ mol^{-1}, which indicates that I$_2$ is very stable (Table 7).

The reaction coordinate for the opening of the transannular bond in the 6/6 closed isomer of C$_{60}$O has been reported at the MNDO and HF/3-21G levels by Raghavachari and Sosa.[29] In order to consider another possible path dissociation of molozonide, which corresponds to the breaking of the C2−O3′ prior to the breaking of the O1′−O2′ bond, we have repeated this kind of calculation. For a set of fixed values of corresponding C2−O3′ distance ranging from 0.16 to 0.24 nm, all the other geometrical parameters were completely optimized at the AM1 level. The resulting energies are listed in Table 8. The opening of C2−O3′ bond is found to be a high-energy process. The structure at C−O = 0.18 nm is 87.6 kJ mol^{-1} higher in energy than the 6/6 PO, on the other hand, the activation energy of breaking O1′−O2′ is only 58.2 kJ mol^{-1}. It can be concluded

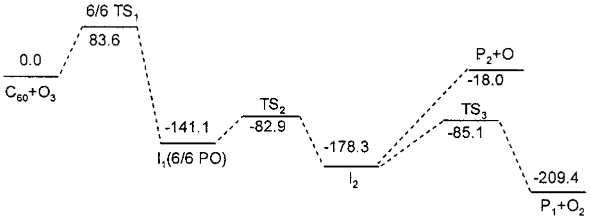

Figure 7. AM1-calculated energy profile for ozonization of C_{60}. The relative heats of formations (kJ mol^{-1}) for all intermediates and transition states are given.

TABLE 9: Bond Length of TS_3 and P_2 (Unit: nm)

	C1−C2	C1−O1′	C2−O3′	O2′−O3′
TS_3	0.1950	0.127	0.1410	0.115
P_2	0.266	0.1218	0.1218	

TABLE 10: Calculated Activation Energy ($\Delta H^{\ddagger}$), Retro reaction Activation energy ($\Delta H^{\ddagger}_r$), Heats of Formation and Heats of Reaction Path 1 (Unit: kJ mol^{-1})

	ΔH_f°	ΔH_r	$\Delta H^{\ddagger}$	$\Delta H^{\ddagger}_r$
I_2 (reactant)	4051.1			
TS_3	4145.4		94.3	124.8
P_1+O_2 (product)	4020.6	−30.6		

from the result that the breaking of C2−O3′ will need more energies than the breaking of O1′−O2′, and this path is impossible.

3.3. Formation of Ozonization Product. The third step of ozonization of C_{60} has two paths. One path (path 1, i.e., reaction III in Figure 2) is that one O_2 molecule, eliminated from I_2 through a transition state, formed $C_{60}O(P_1)$ with epoxide functionality. The other path (path 2, i.e., reaction IV in Figure 2) is one step reaction, i.e., one oxygen atom eliminated from I_2 and formed $C_{60}O_2(P_2)$ with ketone functionality (Figure 6).

It can be seen from the bond lengths of TS_3 (See Table 9) that the distance between C1−C2 is shortening and the bond is formatting gradually. Meanwhile the bond length of C2−O3′ is stretching and O−O is moving away from C_{60}.

It can be seen from Table 10 that the activation energy of path 1 is 94.3 kJ mol^{-1}. The formation of P_2 is through a dissociation of O atom from I_2 and there is not any transition state in this process. The dissociation energy in path 2 is 197.4 kJ mol^{-1}. The heats of formation of P_2 (3776.4 kJ mol^{-1}) is smaller than that of P_1, but from a kinetic point of view we think that the major product of the ozonization of C_{60} is P_1, i.e., $C_{60}O$ with epoxide structure.[33,34] This is in agreement with experimental results.[5−7]

According to the computational results, we obtained the reaction pathways of ozonization of C_{60} (Figure 7).

4. Conclusions

The present results suggest a mechanism for the ozonization of C_{60}. A systematic AM1 semi-empirical method calculations was carried out in the transition states, intermediates, and products involved in which the mechanism have been optimized. The calculations lead to the following conclusions: (1) The addition of O_3 to C_{60} is most likely to have occurred in 6/6 bond. The heat of formation of 6/6 PO is 79.5 kJ mol^{-1} lower than that of 6/5 PO, and the activation energy of 6/6 addition is 50.2 kJ mol^{-1} lower than that of 6/5 addition. It can be concluded that not only from a thermodynamic point of view but also from a kinetic point of view the O_3 was most possible added on the 6/6 bond of C_{60}. (2) The major product of ozonization of C_{60} is $C_{60}O$ with epoxide functionality. (3) The rate-determining step of ozonization of C_{60} is the 1,3-dipole addition of O_3 to C_{60}. The activation energy of the rate-determining step is quite lower (84.6 kJ mol^{-1}), showing that C_{60} is well suited for ozonization.

Acknowledgment. Project 29773022 supported the National Natural Science Foundation of China.

References and Notes

(1) Wood, J. M.; Kahr, B.; Hoke, S. H.; Dejarme, L.; Cooks, R. G.; Ben-Amotz, D. *J. Am. Chem. Soc.* **1991**, *113*, 5907.
(2) Creegan, K. M.; Robbins, J. L.; Robbins, W. K.; Millar, J. M.; Sherwood, R. D.; Tindall, P. J.; Cox, D. M.; Smith, A. B., McCauley, J. P., III; Jones, D. R.; Gallagher, R. T. *J. Am. Chem. Soc.* **1992**, *114*, 1103.
(3) Kalsbeck, W. A.; Thorp, H. H. *J. Electroanal. Chem.* **1991**, *314*, 363.
(4) Malhotra, R.; Kumar, S.; Satyam, A. *J. Chem. Soc., Chem. Commun.* **1994**, 1339.
(5) Heymann, D.; Chibante, L. P. F. *Chem. Phys. Lett.* **1993**, 207, 339.
(6) Deng, J. P.; Mou, C. Y.; Han, C. C. *J. Phys. Chem.* **1995**, *99*, 14907.
(7) Beck, R. D.; Stoermer, C.; Schulz, C.; Michel, R.; Weis, P.; Brauchle, G.; Kappes, M. M. *J. Chem. Phys.* **1994**, 101, 3243.
(8) Criegee, R. *Angew. Chem., Int. Ed. Engl.* **1975**, *14*, 745.
(9) Criegee, R. *Angew. Chem., Int. Ed. Engl.* **1975**, *14*, 765.
(10) Cremer, D. *J. Am. Chem. Soc.* **1981**, 103, 3619.
(11) Hiberty, P. C.; Devidal, J. P. *Tetrahedron* **1978**, *35*, 1015.
(12) Hiberty, P. C. *J. Am. Chem. Soc.* **1976**, *98*, 6088.
(13) Harding, L. B.; Goddard, W. A., III. *J. Am. Chem. Soc.* **1978**, *100*, 7180.
(14) Dewar, M. J. S.; Hwang, J. C.; Kuhn, D. R. *J. Am. Chem. Soc.* **1991**, *113*, 735.
(15) Cremer, D. *J. Am. Chem. Soc.* **1981**, *103*, 3627.
(16) Cremer, D.; Kraka, E.; Mckee, M. L.; Radhakrishnan, T. P. *Chem. Phys. Lett.* **1991**, *187*, 491.
(17) Cremer, D.; Gauss, J.; Kraka, E.; Stanton, J. F.; Bartlett, R. *Chem. Phys. Lett.* **1993**, *209*, 547.
(18) Cremer, D.; Bock C. W. *J. Am. Chem. Soc.* **1986**, *108*, 3375.
(19) McKee, M. L.; Rohlfing, C. M. *J. Am. Chem. Soc.* **1989**, *111*, 2497.
(20) Dewar, M. J. S.; Hwang, J. C.; Kuhn, D. R. *J. Am. Chem. Soc.* **1979**, *70*, 1898.
(21) Ponec, R.; Yuzhakov, G.; Haas, Y.; Samuni, U. *J. Org. Chem.* **1997**, *62*, 2757.
(22) Anglada, J. M.; Crebuet, R.; Bofill, J. M. *Chem. Eur. J.* **1999**, *5/6*, 1809.
(23) Dewar, M. J. S.; Zoebisch, E. G.; Healy, E. F.; Stewart, J. J. P. *J. Am. Chem. Soc.* **1985**, *107*, 3902.
(24) Stewart, J. J. P. MOPAC7, QCPE 455; Indiana University: Bloomington, IN, 1983.
(25) Sola, M.; Mestres, J.; Marti, J.; Duran, M. *Chem. Phys. Lett.* **1994**, *231*, 325.
(26) Dewar, M. J. S.; Olivella, S.; Stewart, J. J. P. *J. Am. Chem. Soc.* **1986**, *108*, 5771.
(27) Zozom, J.; Gillies, C. W.; Suenram, R. D.; Lovas, F. J. *Chem. Phys. Lett.* **1987**, *149*, 64.
(28) Gillies, J. Z.; Gillies, C. W.; Suenram, R. D.; Lovas, F. J. *J. Am. Chem. Soc.* **1988**, *110*, 7991.
(29) Zhang, X. M.; Zhu, Q. Y. *J. Org. Chem.* **1997**, *62*, 5934.
(30) Gonzalez, C.; Schlegel, H. B. *J. Chem. Phys.* **1989**, *90*, 2154.
(31) Kan, C. S.; Calvert, J. G.; Shaw, J. H. *J. Phys. Chem.* **1981**, *85*, 2359.
(32) Mestres, J.; Duran, M.; Solà, M. *J. Phys. Chem.* **1996**, *100*, 7449.
(33) Raghavachari, K.; Sosa, C. *Chem. Phys. Lett.* **1993**, *209*, 223.
(34) Raghavachari, K. *Chem. Phys. Lett.* **1992**, *195*, 221.